Omega-P, Inc.
199 Whitney Avenue, Suite 200
New Haven, CT 06511

Final Report to US Department of Energy

on

Phase I STTR Grant DE-FG02-04ER86193

RF GUN WITH HIGH-CURRENT-DENSITY FIELD EMISSSION CATHODE

Principal Investigator: J. L. Hirshfield
December, 2005

TABLE OF CONTENTS

1. Identification and significance of the problem or opportunity, and technical approach p. 2
   - 1a. Introduction 2
   - 1b. Technical approach 2
     - 1b.1 Available S-band RF gun and beam simulation studies 3
     - 1b.2 Carbon nanotube field emitters 4
       - 1b.2a Design and fabrication of electron multiplier 6
       - 1b.2b Novel carbon nanotube field emitter 7
       - 1b.2c Uniform emission control by resistive layer 7
2. Anticipated public benefits 8
3. Degree to which Phase I demonstrated technical feasibility 8
   - 3a. Introduction to carbon nanotube field emission cathodes 9
   - 3b. Review of goals for Phase I on nanotube cathode fabrication 9
   - 3c. Description of preliminary experiments on nanotube cathodes 10
   - 3d. Results and discussion of preliminary experiments on nanotubes 11
   - 3e. Application of vertically aligned thin multiwall carbon nanotubes 15
   - 3f. Experiments and discussion 15
   - 3g. Field enhancement by space-controlled CNT using nanotemplate 18
   - 3h. Conclusions for Phase I nanotube cathode work 19
   - 3i. Review of goals for Phase I simulations of field emission cathode 19
   - 3j. Results of simulation studies of field emission cathode in RF gun 20
   - *References* 25

1. IDENTIFICATION AND SIGNIFICANCE OF THE PROBLEM OR OPPORTUNITY, AND TECHNICAL APPROACH

1a. Introduction

The DoE 2004 SBIR/STTR Phase I Program Solicitation requested grant applications under Topic 5c *Inexpensive High Quality Electron Sources*, where ideas were sought for novel RF gun technologies operating at output electron beam energies >3 MeV. A related requirement was implicit within Solicitation Topic 6b on *Radio Frequency Power for Linear Accelerators*, on novel concepts for sources of RF power to drive a future electron-positron collider. The project discussed in this report relates to this second requirement; since the advanced high-current-density field emission cold cathodes being developed for RF guns could be modified for use in a wide variety of cold-cathode diode guns for high-power klystrons, magnicons, and other rf sources. In response to the Topic 5c in the 2004 Solicitation, Omega-P, Inc. proposed and was awarded a Phase I STTR grant DE-FG02-04ER 86193 "RF Gun with High-Current-Density Field Emission Cathode." Under this project, design and development of a novel high-current-density field emission cold cathode was initiated. This cathode was to have been designed for evaluation in an existing 2-1/2 cell S-band RF gun with associated instrumentation that is installed at the Yale University Beam Physics Laboratory, and that is available to Omega-P. Building prototype field emission cathodes, testing of these cathodes in the RF gun, and measurements of parameters of the electron beams generated, would have been carried out during Phase II. However, the Phase II grant was not awarded.

This project was structured as an STTR grant, since significant collaboration between Omega-P, Inc. and Florida International University (FIU) was involved. In particular, Omega-P conducted simulations studies to determine current density and geometrical requirements for the cathode that are consistent with the existing RF gun and, in Phase II, would have conducted laboratory tests of the RF gun; while FIU designed and developed the high-current-density field emission cold cathodes themselves. This collaboration was built upon Omega-P's expertise in high-power microwave aspects of accelerator physics, including many years of operation of its 6-MeV S-band RF gun with a thermionic cathode; coupled with FIU's expertise on high-current-density carbon nanotube field emitters. Omega-P and FIU closely coordinated their respective tasks and work jointly to analyze the results and plan future steps.

RF guns are ubiquitous as injectors at many electron accelerators, often operating with laser photocathodes that can produce bunches a few picoseconds (ps) in width with of the order of 10^{10} electrons/bunch (1.6 nC), corresponding to peak currents exceeding 100 A. Thermionic cathodes are also used in RF guns; for example at SRRL where 70 pC, 4 ps bunches have been produced using an alpha-magnet/buncher after the S-band RF gun. (S. Park and J.N. Weaver, paper MOP66, linac96) Thermionic cathodes are also useful in RF guns when a pulsed train of many bunches is needed: the 6-MeV S-band gun available to Omega-P is capable of generating a train of ~3000, ~250 pC bunches spaced by 350 ps in a 1-μs-wide pulse with a repetition rate of 10 Hz. Several factors limit the charge/bunch that can be obtained from an RF gun, including the emission current density capability of the cathode; for long-life operation thermionic cathodes are usually limited to current densities not exceeding 10 A/cm^2; it is about 1.5 A/cm^2 in the above-cited SSRL gun. However, since current density (in the absence of undesired ion space-charge compensation) is fundamentally limited by Child's Law, high enough RF electric fields are required across the anode-cathode gap to extract the maximum available current

density. Design of the cells of an RF gun must invoke optimized simulations of self-consistent space-charge flows in order to allow extraction of the highest available current, while maintaining the lowest possible beam emittance and energy spread.

Thermal expansion and lifetime are also critical issues with cathodes in RF guns. For thermionic cathodes, uneven thermal expansion can misalign the cathode with respect to the surrounding cavity structure, thus introducing asymmetric emission and increased beam emittance. A similar issue arises in conventional diode electron guns (as used in high-power klystrons and magnicons) in which the cathode must be centered precisely with a narrow gap between it and a surrounding focus electrode. Thermal expansion can alter this gap spacing and/or cause cathode tilting, again leading to variation in gun perveance and/or asymmetric emission and diminished beam quality. Evaporation of cathode material onto surrounding electrodes is also a problem in hot-cathode guns. Obtaining accurate thermal analysis for the complex geometries in these guns is not simple, often resulting in practice in less-than-ideal beam quality, diminished device performance, and diminished lifetime. Cold cathode operation will allow avoidance of issues arising from thermal expansion and evaporation, and may also allow exceptionally-long lifetimes, since negligible emitter material is consumed during cathode operation, as in oxide cathodes; and since the novel cathode construction can provide shielding of the carbon nanotube field emitters from returning electrons that are unavoidable in RF guns and that are an important caused of limited cathode longevity.

New understanding and implementation of advanced laboratory techniques have recently allowed fabrication of carbon nanotube (CNT) field emitters that show great promise as cathodes in high-power RF devices, including RF guns. Field emission sources have not proven practical in earlier attempts to incorporate them into high-power device cathodes, due to their fragility and susceptibility to destruction from ion bombardment and/or unavoidable vacuum arcs during gun conditioning. But the novel approach described here for utilizing cold cathode field emission CNT′s, coupled with secondary current channel multiplication in a outer barrier that can protect the CNT′s, offer new opportunities for building improved cathodes for many vacuum electronics applications, including improved high-current RF guns for accelerator injector applications. An additional highly-attractive feature of the cold cathode field emission cathode described here is the possibility of rapid gating and/or RF modulation of the emission using built-in gate junctions at the base of each CNT.

1b. Technical Approach

The technical approach for this STTR project includes three major aspects: (*a*) analysis of RF gun beam dynamics in the available S-band rf gun for arbitrary current density as high as several kA/cm^2, as could be available from a field emission cold cathode; this analysis is expected to lead to specifications for cathode current density and cathode geometry compatible with the available RF gun; (*b*) development of specific fabrication steps needed to construct the cathodes specified in task (*a*), and (*c*) organization of an aggressive Phase II laboratory program for production of a variety of cathodes for installation and testing in the RF gun during Phase II.

1b.1. Available S-band RF gun and beam simulation studies

Omega-P has, for nearly a decade, operated a 2-1/2 cell thermionic cathode RF gun that can produce a train of ~3000, ~250 pC bunches spaced by 350 ps in a 1-μs-wide pulse with a

repetition rate of 10 Hz. A diagram of the RF gun, with the cathode structure removed, is shown in Fig. 1. This gun has supplied a 6-MeV beam used in experiments on the synchrotron radiation maser, on the inverse free-electron laser accelerator, and on dielectric wake field studies. The field emission cathode to be built and tested under the proposed project is to mate with the mechanical, electrical, and electrodynamic features of this existing structure. A former SLAC XK-5 klystron, modulator, and associated S-band rf infrastructure for this rf gun are also available to Omega-P. Analysis of space-charge limited beam formation in this gun geometry is carried out using available steady-state and time-dependent trajectory codes, assuming various levels of available current density at the cathode surface, so as to characterize the properties of the beam that is produced and accelerated in the gaps of the gun. These simulation studies help determine the selection of cathode dimension and "focus electrode" geometry near the cathode, so as to provide a low-emittance beam with desired charge and energy.

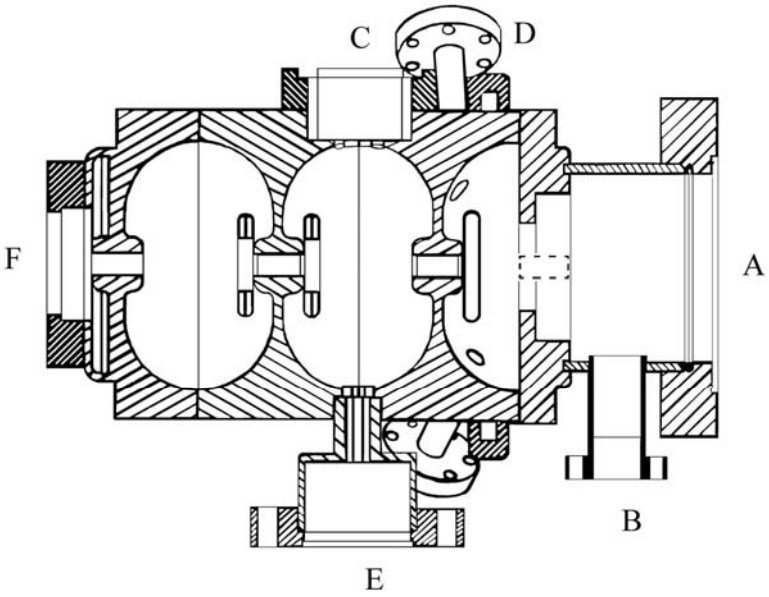

Fig. 1. Diagram of 2-1/2 cell S-band rf gun, with cathode assembly removed.
A – flange for mounting cathode assembly; **B** – port for cathode electrical connections; **C** – waveguide rf power input; **D** – cathode viewing port (one of two); **E** – ion pumping port (one of two); **F** – beam exit port. Dashed outline at flat face of right-most rf half-cell shows approximate location of field emission cold cathode being designed in this program.

1b.2. Carbon nanotube field emitters.

The potential for high emission current density has always been an attractive feature of field emitters. For microwave vacuum electronics applications, high total current and durability are crucial requirements. So far, the highest total field emission current has been 0.1-0.8 A [1]. CNT emitters demonstrated a relatively large current density, as high as 4 A/cm^2 [2]. This result was obtained from randomly distributed CNT emitters within a small area, with only a small fraction of total available nanotubes participating in the electron emission. A realistic practical challenge is to demonstrate a total current exceeding 10 amps from an emitting area of 1 mm^2. In order to increase the total emission current density, many emitters should operate

simultaneously with maximum field enhancement. To meet those requirements, powerful emitters which are uniform and capable of high current emission and yet are robust enough to endure an intense field emission environment and an RF environment are needed.

Novel device design for ultra high current density together with strong protection against arc damage and ion bombardment are being developed in this project to maximize the emitter performance and reliability. Strong fields present in guns for high power beams will accelerate ions towards the cathode, leading to erosion and finite cathode lifetime, while unavoidable gun arcs can lead to irreversible cathode damage. We are developing a unique design, shown in Fig. 2, in which an electron multiplier is placed on top of the emitters to increase the electron current density and protect the cathode from plasma puffs, arcing, and reflected electrons. The solid ceramic structure of the electron multiplier is to act as a rugged shield, providing significant protection of the nanotubes against hostile events. The inability of field emitter arrays (FEAs) to emit uniformly or to achieve a linear scaling of emission current with array size is due to the exponential relationship between current and voltage. The exponential part of the Fowler-Nordheim equation contains both the field enhancement term and the work function term. Small changes in field enhancement, i.e. tip sharpness or emitter height, and changes in the local work

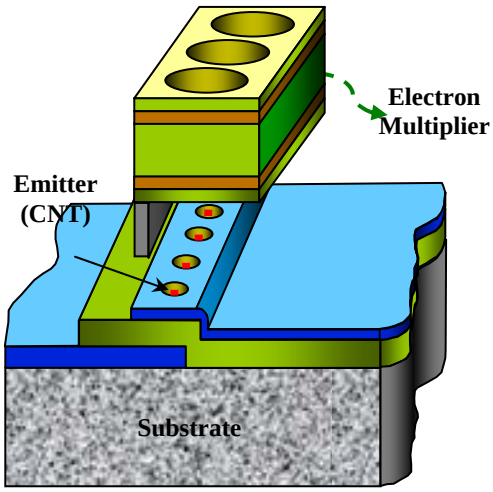

Fig. 2. Schematic of a proposed novel cold cathode for high current density including carbon nanotube emitters and electron multiplier.

function due to adsorbates cause exponential changes in emission current. Even in the best-made arrays, the sharpest, cleanest, and tallest tips emit first, and most of the current is produced from a very small percentage of tips. However, as the potential is increased these overburdened tips will fail catastrophically before the rest of the tips can contribute any significant current. A major limitation to the application of field emitters is the lack of emission stability. Fluctuations in emission current by a factor of more than two are common for most emitters not operating under ultra-clean, ultra high vacuum conditions. This is not only due to the constituents of the given vacuum, but also the instability of the emitter materials themselves while subjected to high fields and currents. Novel electron multiplier and high surface resistance emitters together with novel materials and device design can make possible the next generation of high current sources; and it is towards these improvements that this project is aimed.

1b.2a. Design and fabrication of electron multiplier. We are developing a unique design that involves placing an electron multiplier on top of the emitters to increase the electron current density and protect the cathode from plasma puffs, arcing, and reflected electrons that are inevitable in high beam current devices. The extra operational flexibility that the electron multiplier gives will also allow improve emission uniformity by introducing a controlled space-charge region just above the CNT emitters. A rough estimation of current density available from a periodic carbon nanotube array yields a value exceeding 100 A/cm^2, as will be discussed below. However, in consideration of realistic variation of materials behavior and non-ideal situations, we propose to have a follow-on process to boost the emission current using the high secondary electron emission from some materials. The proposed electron multiplier is an array of individual channel multipliers, operated by avalanche multiplication of secondary electrons. When incident electrons from the electron emitters strike the internal walls of the channel, secondary electrons are emitted from the surface. The FIU team and its collaborators have already observed that the secondary electron emission (SEE) yield increased enormously when electrons bombarded a very thin (~15-30 nm) MgO film deposited on highly conductive carbon nanotube surface [3]. The SEE yield as a function of the bias potential shows the emission yield can be as large as 15,000 secondary electrons per incident primary. It has also been reported that this current amplifier allows an increase of the field emitter array current (FEA) by at least 10 times, even in the high emission current regime [4]. The multiplier is based on high secondary electron yield materials, such as MgO, BeO, SiO_2 and CVD diamond. Important aspects to consider in the design of electron multipliers include the efficient transport of charge as the secondary electrons are emitted, and heat dissipation to allow prolonged and repeated use.

It is planned to first coat the inside surface of the channel wall with highly conductive material layer (such as electrodeless plated or sputtered Cu [3,4]), as shown in Fig. 3. We will

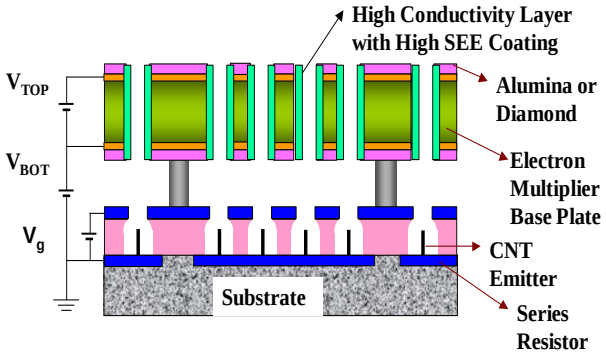

Fig. 3. Schematic illustration of electron multiplier placed over CNT cathodes.

then provide a very thin (~5 – 30 nm) coating of SEE material over the conductive layer by sputtering, CVD or sintering of a thin green powder layer. Various multiplier structural designs listed below will be investigated to understand and achieve significant current amplifications as needed, e.g., by a factor of 10 – 100. Because of a highly conductive layer placed underneath the thin SEE coating, charge build up during secondary electron emission will be avoided. Electrical conductivity of the conductive layer is sufficiently high to allow charge bleed off at a rate higher than the charge collection rate.

The strong fields present in high current guns will accelerate ions towards the cathode, leading to erosion and finite cathode lifetime, while unavoidable gun arcs can lead to irreversible cathode damage. It can be anticipated that exposed nanotubes might be seriously damaged—even destroyed—by ion bombardment and/or gun arcs. But the solid ceramic structure of the electron multiplier should act as a rugged shield, providing significant protection of the nanotubes against such hostile events. To reduce charging of the multiplier surfaces, and the possibility of breakdown, the multiplier surfaces will be coated with a semiconductive hard layer such as diamond, deposited by chemical vapor deposition (CVD). The assembled electron multiplier will be tested in high rf fields using S-band rf facilities available to Omega-P.

Practical utilization of a high current density cathode is not an easy matter since the space charge limited current density from any electron source cannot exceed the Child's Law limit (unless undesired ion space-charge compensation is present as in a less reliable, poor vacuum environment). Careful considerations of designs and measurements need to be carried out. A rough estimate from Child's Law indicates that a high current cathode capable of 1 kA/cm^2 emission density can be operated in the space-charge limited regime using a 2.5 cm effective gap at ~0.5-1.0 MV to produce a bunched beam with peak power in the GW range. Fields up to ~100 MV/m are routinely established without breakdown in rf guns.

1b.2b. Novel carbon nanotube field emitter. Due to their high conductivity, nanometer diameter, unique structure and chemical stability, CNT′s are an ideal candidate for electron field emission devices. In contrast to conventional emitters, CNT′s exhibit a lower overall threshold electric field and higher current density. It has been reported that each CNT is capable of producing emission current in excess of 1 μA [6]. Careful control of nanotube configurations and uniformity, for example as an array of vertically aligned nanotubes 0.3 μm tall and 0.3 μm apart, would give ~10^9 CNT′s/cm^2, and hence the total current density could reach ~1000 A/cm^2, provided that one can cause most of the nanotube emitters to participate simultaneously. It is therefore essential to thoroughly control the geometry and uniformity of nanotubes in order to ensure that the maximum field emission capability is utilized. We propose to carry out investigations for understanding and control of nanotube geometry, ohmic contact, and surface modification as described below.

1b.2c. Uniform emission control by resistive layer. The possibility of integrating devices such as passive series resistors and/or active field effect transistors (FETs) with field emitters will be investigated. Preliminary analysis of the problem shows that the usefulness of such passive and active control might be somewhat limited for high-current field emitters. Nevertheless, this highly promising approach for self-regulation of CNT emission deserves careful study before its full utility can be gauged. In addition, the possibility will be examined of modulating or chopping the emission current using an external synchronized rf low-voltage signal on the base of the CNT emitters; it is conceivable that such a strategy would allow emission into the rf gun during only a fraction of each rf cycle, thus producing beam bunches whose duration would be shorter than otherwise, perhaps in the few-ps range as in laser photo-cathodes.

2. ANTICIPATED PUBLIC BENEFITS

Cathode technology is considered to be the Achilles heel of vacuum electronics devices, since the quality of the electron beam that can be extracted from a cathode in an electron gun is more sensitive to the cathode than to any other element in the gun. Moreover, the lifetime of the vacuum electronics device is more often than not given by the lifetime of the cathode. Thus, any promising new technology for replacing conventional cathodes in vacuum electronics devices could bring significant benefits to the technological, scientific, and public communities. The present project is for development of a novel cold cathode that embodies field emission from many carbon nanotubes, with the emitted current from each nanotube amplified in an adjacent channel secondary emission multiplier. Insertion of a series field emission transistor at the base of each nanotube would allow high-speed modulation and/or regulation of the emitted current, and sturdy construction of the ceramic element containing the channel multipliers would provide protection of the nanotubes from inadvertent—but unavoidable—returning ions and/or vacuum arcs that can cause irreversible damage. The thrust of this project was to design a field emission cold cathode suitable for installation in an existing 2-1/2 cell S-band rf gun, since this would provide a low-cost test bed for the gun, in high-enough rf electric fields to realize emission current densities approaching 1 kA/cm^2. Other uses for such a cathode can be found in diode guns for high-power amplifiers used in accelerator applications, such as klystrons and magnicons, thus possibly eliminating many technical issues that arise from use of a thermionic cathode. Furthermore, the capability of the carbon nanotubes to be rapidly gated or modulated using a transitor at the base of the nanotube could provide remarkable improvement in cathode technology, benefiting not only RF guns (where dependence upon costly and delicate lasers for cold cathode emission is now wide-spread), but as gated emitters in other vacuum electronics devises, such as klystrons. All of these potential benefits that could flow from the R&D described here could lead to lowered costs and higher reliability for future vacuum electronics devices, both in scientific applications and in commercial uses.

3. DEGREE TO WHICH PHASE I DEMONSTRATED TECHNICAL FEASIBILITY

The main goal of the overall Phase I and Phase II project was to develop rugged, long-life high-current-density, cold cathodes for high power RF guns, to be used as injectors for electron accelerators; and in guns for high current RF amplifiers (such as klystrons and magnicons) needed for future accelerator applications. The key features to be developed in this project invoke use of carbon nanotube (CNT) field emitters (yielding perhaps 1 μA each) in an array shielded by a rugged ceramic containing secondary emission channels capable of multiplying each beamlet up to a level of about 1 mA. With an emitter array density of $10^5 – 10^6$ cm^{-2}, the resulting current density is 0.1 – 1.0 kA/cm^2. Microcircuits built in to each CNT are being developed to provide current regulation and rapid current modulation or chopping, so as to narrow the phase window for injection of electrons into the first half-cell of the RF gun. New analysis and simulation of the behavior of RF guns with cathodes capable of kA/cm^2 emission current density has been carried out, to assist in setting specifications for the cathodes to be built, and to anticipate the properties of the beams that can be produced. In this section, reports are given of progress during Phase I towards achievement of these goals.

3a. Introduction to carbon nanotube field emission cathodes

Carbon nanotubes, which are cylinders of graphene sheet, have great promise as material for field emitter cathodes in high-power RF devices, including RF guns. [1, 2] Field emission sources have not proven practical in earlier attempts to incorporate them into high-power device cathodes, due to their fragility and susceptibility to destruction from ion bombardment and/or unavoidable vacuum arcs during gun conditioning. But the novel approach we have suggested for utilizing cold cathode field emission carbon nanotubes (CNT′s), coupled with secondary current channel multiplication in a outer barrier that can protect the CNT′s, offer new opportunities for building improved cathodes for many vacuum electronics applications, including improved high-current rf guns for accelerator injector applications.

The CNT as a field emitter should satisfy the following conditions: high conductivity, high aspect ratio (length/diameter), and high mechanical strength and easy to process. Carbon nanotubes having small diameter and large length are suitable for field emission materials. The electric field on the tip changes significantly with the geometry of the tip which is related to the aspect ratio. Sharp tips with high aspect ratio can help electrons to tunnel through the barrier. Since single-wall carbon nanotubes (SWNTs) have high aspect ratio and small radius of curvature (~ 1 nm), they have been reported to show large field enhancement factor, low threshold voltage, and high emission current [3]. However, the degradation of emission current with time is an obstacle for the application of SWNTs as field emitters [4]. We have synthesized vertically aligned thin MWNTs for the longevity of field emitter, by using $Fe/Mo/Al_2O_3$ nanoparticles as catalyst. The average diameter of synthesized MWNTs is approximately 10 nm. The measurement of field emission properties of vertically aligned thin MWNTs using diode structure showed high emission current, low turn-on voltage, and high field enhancement factor. As the distance between two carbon nanotubes is small, the electrical field gradient on the emitter tips is greatly reduced, which will affect the electron emission, this effect is called field screening effect. To overcome the field screening effect, we need to control the distance of carbon nanotubes. Therefore, to produce the most effective field emission cathodes, an array of aligned and spacing controlled carbon nanotubes are needed. We have designed and prepared the fabrication process of a secondary electron amplifier in order to multiply the current density obtained from carbon nanotubes, and to avoid cathode destruction from ion bombardment and/or unavoidable vacuum arcs during gun operation.

3b. Review of goals for Phase I on nanotube cathode fabrication

Synthesis of vertically aligned thin multiwall carbon nanotubes (MWNT's). Compared to single-wall nanotubes, MWNT's show longer lifetimes, which is related to their superior mechanical properties. However, the large diameter of MWNT's results in poor field emission properties, such as lower current density with small field enhancement factor [5, 6]. In order to improve field emission properties of MWNT's, only thin MWNT's are studied in this project.

Growth of vertically aligned thin multiwall carbon nanotubes. The main goal of this set of tasks is to grow aligned carbon nanotubes using an anodic alumina oxide (AAO) template. The advantage of this method is that densely aligned ordered carbon nanotubes with large aspect ratio are obtained (Fig. 3). Fulfillment of this goal includes growing aligned carbon nanotubes with different spacing and characterizing their field emission properties; increasing the field emission

current density up to 10 A/cm^2 (before amplification); and finding the optimum catalyst deposition conditions.

Design and Fabrication of Micro Channel Plate. The goals of this set of tasks are fabrication of MCP with alumina and AAO having high aspect ratio; experimental and theoretical determination of the geometry of electron multiplier channel for high secondary electron emission; develop techniques for avoiding space charge by adding channel hole coating and by changing pulse operation mode; and design of MCP structure for high heat dissipation operation.

3c. Description of preliminary experiments on nanotube cathode fabrication

Synthesis of vertically aligned thin multiwall carbon nanotubes. Niobium (Nb) thin films with a thickness of 200 nm were deposited on SiO_2/Si substrate by DC magnetron sputtering. Catalyst solution was prepared with iron (III) nitrate nonahydrate ($Fe(NO_3)_3 \cdot 9H_2O$,40mg), bis(acetylacetonato)-dioxomolybdenum (VI) ($MoO_2(acac)_2$, 3mg), Fe:Mo molar ratio was about 10:1. And aluminum oxide nanoparticles (30, 15, and 7.5 mg) were used as catalyst supporter. The catalyst particles were dissolved in methanol (30 ml) and sonicated for 30 minutes to form suspension. A couple of drops of the catalyst solution were dropped onto Nb/SiO_2/Si substrate. The prepared substrate was loaded in a quartz tube CVD-reactor, followed by drying at room temperature for 10 min, baking at 160 ^oC for 5 min, and heating to 700 ^oC in Ar atmosphere. After the temperature was stabilized at 700 ^oC, Ar gas flow was replaced by C_2H_4 for the synthesis of MWNTs. C_2H_4 flow was maintained for 30 minutes. After the synthesis, the reactor was cooled with Ar flow to room temperature.

Characterization. Scanning electron microscopy (SEM) was used to investigate the morphology of vertically aligned thin MWNTs. Micro-Raman spectroscopy (focusing area: 5μm in diameter), using laser excitation wavelength of 785 nm, was used to examine the degree of graphitization. The diameters of the MWNTs were measured using transmission electron microscopy (TEM). During this project, field emission system which has vacuum system up to 10^{-7} Torr was developed. The system and its measurement schematic are shown in Fig. 1. The measurements were done using a DC power supply and the maximum current obtained was as high as 2.5 mA.

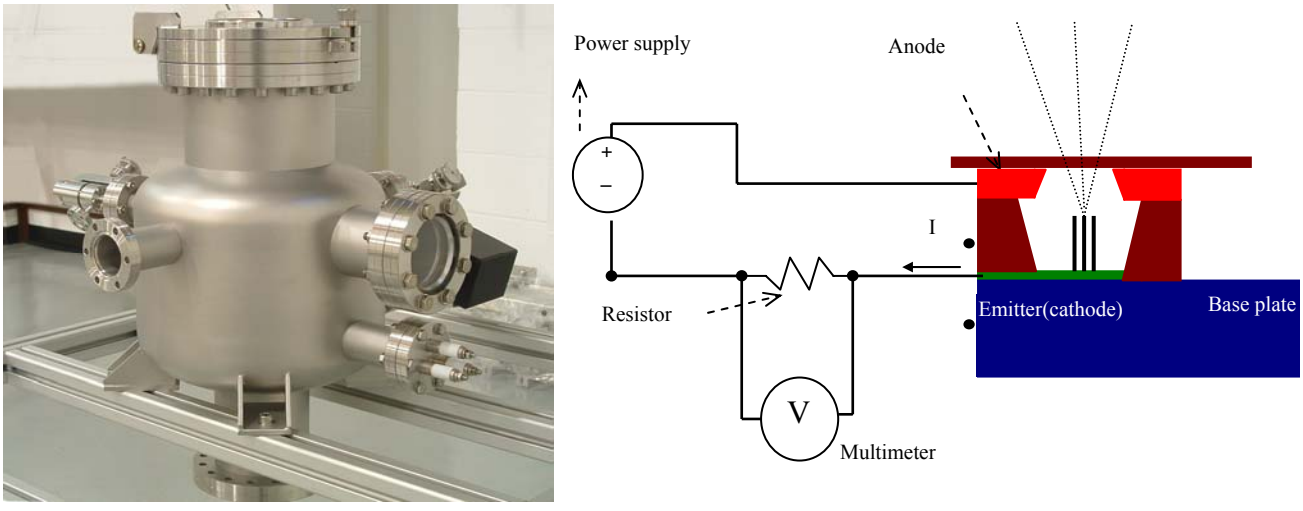

Fig.1. Field emission system prepared during Phase I. (a) test chamber; (b) measurement schematic.

3d. Results and discussion of preliminary experiments on nanotube cathode fabrication

As mentioned above, aluminum oxide (Al_2O_3) nanoparticles were used as supporter for Mo/Fe catalyst particles. Figs. 2 shows the SEM images of carbon nanotubes grown using Mo-doped Fe particles supported by 30 mg, 15 mg, and 7.5 mg of Al_2O_3 nanoparticles, respectively. The density of carbon nanotubes is controlled by the concentration of catalyst solution. With same amount of catalyst salt, when the catalyst supporter decreases, the concentration of catalyst increases. As a result, when Al_2O_3 nanoparticles is decreased to 7.5mg, the density of carbon nanotubes is increasing, which is favorable for vertical alignment. But if the amount of Al_2O_3 nanoparticles is decreased below 7.5mg or increased above 7.5mg, carbon nanotubes are not produced uniformly all over the substrate. It is worthwhile to notice that the diameter of carbon nanotubes is related with catalyst size. With less amount of supporter, larger catalyst clusters are formed. As a result, large diameter nanotubes are grown. So 7.5mg Al_2O_3 nanoparticles is the optimum amount for vertically thin MWNTs growth (Fig 2). From the SEM images, the average length of carbon nanotubes was measured to be around 15 μm.

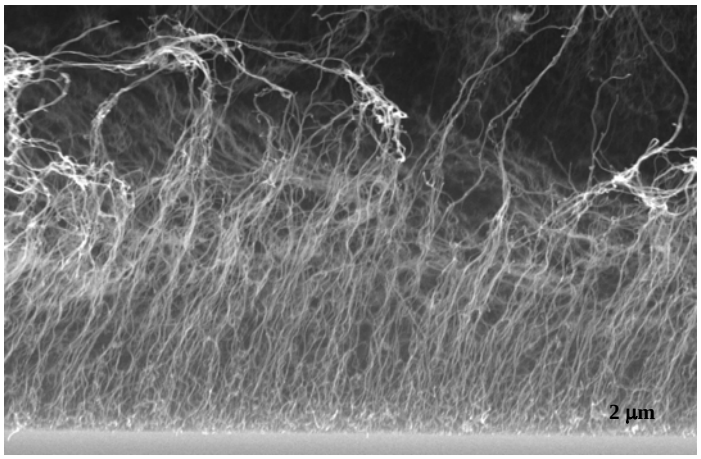

Fig. 2. SEM images of thin MWNTs. The spacing and height of the MWNT's will be made uniform during Phase II using a nano-scale template to position the aluminum oxide nanoparticles catalysts.

Carbonaceous particles were observed scarcely, indicating high purity of MWNTs. The average outer diameter is approximately 10 nm with a range from 7 to 15 nm. Since the average length was found to be 15 μm, the aspect ratio is as high as 1,500. The diameter of innermost walls is from 2.5 to 5 nm. Fig.4 represents Raman spectra of thin MWNTs obtained using laser excitation wavelength of 785 nm. Tangential G-band located at around 1590 cm^{-1} indicates the formation of grapheme sheets. Relatively large D-band peak was observed around 1300 cm^{-1}. The D-band peak has been known to be due to carbonaceous particles, defects in the curved graphene sheet, tube ends, and finite size of crystalline domains of the tubes. Although we have observed very few carbonaceous particles from the SEM and TEM analysis, a large intensity of D-band peak was detected in Raman spectra. This may be due to low temperature growth of MWNTs (~700^{o}C), which does not provide sufficient thermal energy to anneal CNTs to perfect crystalline structure. The inset figure (Fig.4) shows the radial breathing mode (RBM) peaks. Although RBM peaks are not generally observed in MWNTs, we could observe the peaks from our MWNTs sample because of thin diameters. The RBM peaks range from 40 cm^{-1} to 100 cm^{-1}. The numbers shown in the inset denote the diameters of nanotubes, calculated from the relation d_t [nm] = 248 cm^{-1}nm / ω_{RBM} [cm^{-1}] where d_t and ω_{RBM} are diameter of nanotube and wavelength

of RBM peak, respectively. The peaks located below 40cm^{-1} cannot be detected owing to strong Raleigh scattering. The diameters determined from RBM peaks ranged from 2.68 to 5.06 nm, in good agreement with the diameters of innermost walls obtained by TEM measurements.

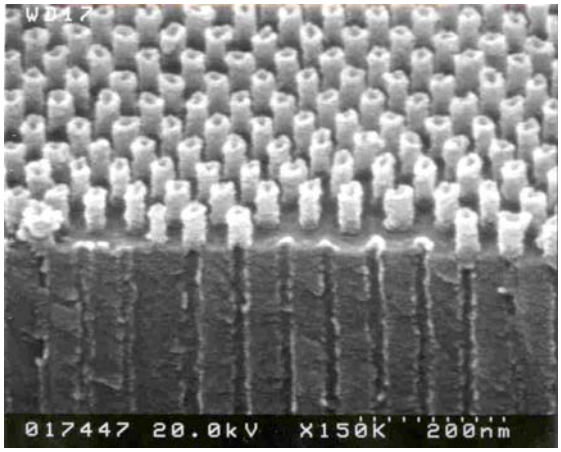

Fig. 3. SEM image of growth of periodic array (height and space controlled) CNTs with a nanotemplate.

Fig. 3 shows carbon nanotube array grown in a nanotemplate (AAO). The diameter and length of the nanotubes are controlled by the geometry of the aluminum oxide template. The nanotubes grown from the AAO nanotemplates duplicate the order and pore diameter of the template, which is determined via the applied voltage during the anodization process. The growth of nanotubes stops at the openings of the pores, because the precursor gases may not decompose so effectively in the absence of the catalytic AAO pores. Thus the carbon nanotube arrays grown by nanotemplate (AAO) exhibit high density and uniformity, with the diameter and length of the carbon nanotubes determined, by the pore diameter and thickness (or depth) of the AAO layer. In order to control the selectivity of the CNT growth, a film (SiO_2, Ni etc) can be deposited on the AAO template, patterned lithographically, and then lifted off. Photolithographic and electron beam lithographic techniques can be used to define selective areas of CNT growth [7].

The field emission data obtained from the vertically aligned thin MWNTs are demonstrated in Fig.5. The measurement was carried out using a diode structure. Indium tin oxide glass (ITO) (anode), separated from the bottom layer of nanotubes (Cathode) by a slide-glass spacer with a thickness of 160 μm. The chamber was maintained 1.0×10^{-6} Torr during the measurement. The bias applied between Nb film (Cathode) and ITO glass (Anode) was from 0~400 V. The turn-on voltage in which current starts increasing is 80 V, which is corresponding to 0.5 V/μm. Emission characteristics were analyzed by Fowler-Nordheim (F-N) plot. The total current I as a function of the local electric field at the emitter surface E_l is given by $I \propto (E_l^2/\phi)\exp(-B\phi^{3/2}/E_l)$ where B is constant (6.83×10^{-9} V eV$^{-3/2}$ m^{-1}) and ϕ is the work function of emitter . The local electric field (E_l) can be related to the field enhancement factor (β) and macroscopic field (E_m) by $E_l = \beta E_m$.

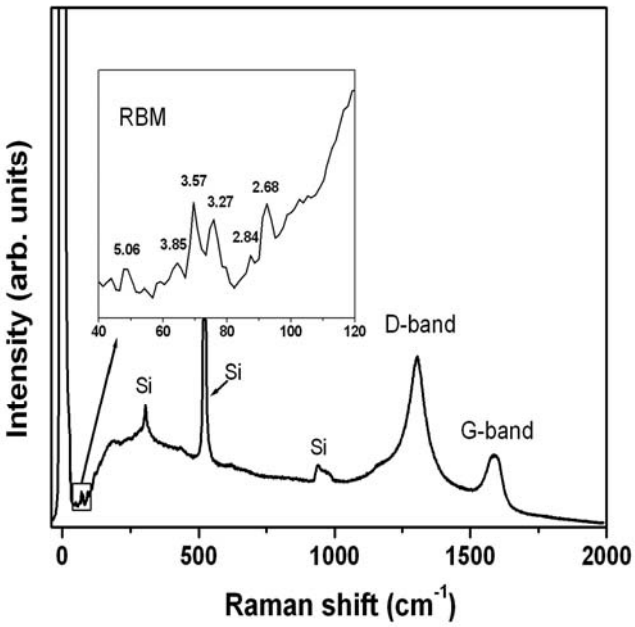

Fig. 4. Raman spectra of thin MWNTs (Laser excitation wavelength of 785 nm)
(Using new facility at FIU, thin MWNTs are grown. During Phase II, aligned single wall and thin multiwall will be synthesized)

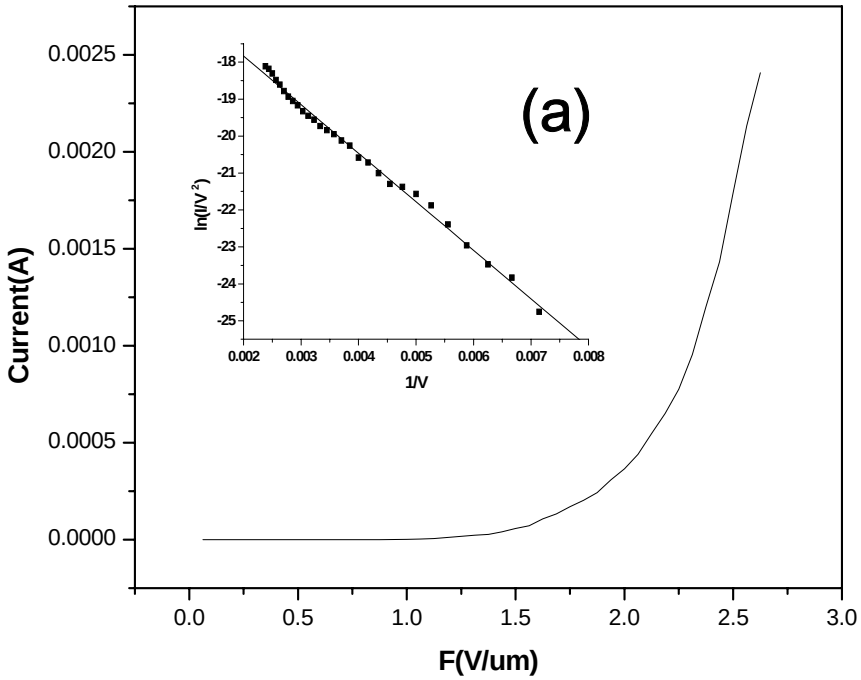

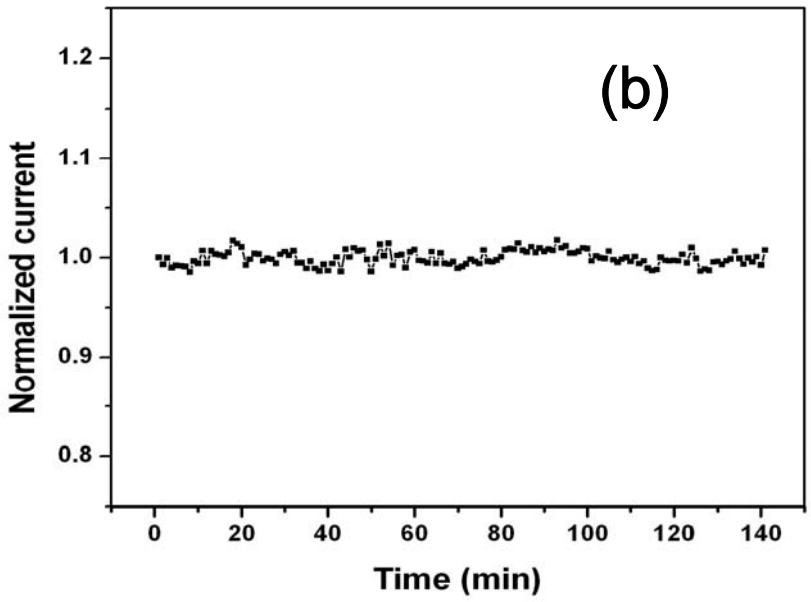

Fig. 5. (a) Field emission I-V curve, inset: Fowler-Nordheim plots.
(b) Current stability. (Field emission was measured at low voltage within a small defined area of 1 mm^2)

The field enhancement factor can be determined from the slope of the F-N plot, i.e. $\ln(I/V^2)$ *versus* V^{-1}, if the work function of the emitter is known. The slope S of the F-N plot is equal to $S = -B\phi^{3/2}d\beta^{1}$ where d is the interelectrode distance (thickness of a spacer). F-N plot converted from the measured I-V data is presented in inset of the Fig. 5a. The measured data fitted well to F-N equation, meaning that the electrons were emitted by field emission mechanism. By assuming the work function of carbon nanotubes to be 5 eV that is the same as that of graphite, the field enhancement factor is determined to be as high as 9,296. This means that the electric field at the location where the nanotubes are emitting electrons is 9,296 times stronger than the applied macroscopic field. This value of field enhancement factor (β) is much higher than the previously reported β of MWNTs, ranging from β =1000 to 5,000 [8-11]. The previously reported diameters of MWNTs were in the range of 20 to 50 nm. Therefore, such a high field enhancement factor of our emitters is believed to originate from thin wall structure of the MWNTs which has high aspect ratio and small diameter. Fig. 5b represents the current stability of field emission current. The emission current density was not decreased even after 140 min at DC bias of 400 volts, indicating good durability of thin MWNTs-emitters. The average emission current fluctuation is less than 2 %.

Low turn-on field of 1 V/μm and high field enhancement factor of 9,296 were obtained from the field emission measurements, which resulted from thin wall structure of the MWNTs with small diameter. Substantial current stability with little fluctuation was also observed. It is suggested that the thin MWNTs can be utilized as a high performance field emission source with high durability and low turn on voltage.

3e. Application of vertically aligned thin multiwall carbon nanotubes with MCP

Microchannel plate (MCP) is an array of microscopic channels with typical channel diameters of 1-100 μm, aspect ratio of 40-100 and axis normal or biased at a small angle (5^o-8^o). MCP is used in high efficiency field emission displays [12], pulse counting applications requiring fast response, good temporal resolution and tolerance to strong magnetic fields [13]. The present project is intended to improve the current density for application in high power microwave devices such as RF guns using carbon nanotubes as electron beam source (cathodes). A MCP can provide a gain (output to input current ratio) of 10^6 depending on the aspect ratio of the channels.

Currently the main material for manufacturing MCP is lead-silicate glass. It is a good material for MCP but it has many disadvantages, such as

- Large parameter deviation and low repeatability of MCP due to possible glass irregularities
- Spottiness of the image due to the difference of thermal histories of the elements of the MCP block
- It is difficult to produce large area MCP [14].

Therefore Alumina (Al_2O_3) or anodized aluminum oxide coated with Magnesium oxide (MgO) can be used as a material for MCP due to its various advantages, such as

- They produce clean ceramic surfaces suitable for high vacuum applications
- Chemical stability of Alumina preserves the properties of MCP in alkali atmospheres
- Not influenced by magnetic fields
- Theoretically 10^{10} channels per sq. cm can be produced in case of AAO [15].

3f. Experiments and discussion

MCP can be made from alumina by micro-drilling of alumina green bodies or using AAO technology [16]. A ceramic green body is a mixture of ceramic powder with appropriate binder and has hardness much lower than sintered form. For the initial experiments MCP will be prepared by micro-drilling of alumina green bodies using CNC drilling machine with a high speed air spindle. Green alumina bodies with micron size diameter holes are then stacked, laminated and sintered to obtain MCP. Fig. 6 shows a MCP and Fig.7 the sintering cycle. When electrically charged particles of sufficient kinetic energy hit the surface of a solid, the later emits electrons. These electrons are called secondary electrons and the bombarding electrons are called primary electrons. For most materials the number of secondary electrons generated by each primary electron (the secondary emission coefficient) lies between 0.2 and 3. Generally the maximum value of metals is about 1 and an insulator is 3 [17]. Fig. 8 shows the cross-sectional view of an MCP channel. The channel wall of an MCP is coated with an electron emissive layer which is formed over a diameter is reduced by 20-30% after sintering and coating of Cu & MgO on the channel walls i.e. 10 μm diameter holes will be achieved after sintering (8% reduction) and coating the channel walls with Cu (10-15 μm) & MgO (5-10 μm) from a mechanically drilled 50 μm diameter holes) resistive layer. Emissive layer is responsible for generating secondary electrons upon bombardment by primary electrons. Resistive layer replenishes the electron deficiency produced in the emissive layer. Cu and MgO are being used as resistive and emissive layer respectively, in the current MCP. The deposition of MgO will be done by techniques such as sputtering and solgel, Cu by electroless Cu solution and sputtering.

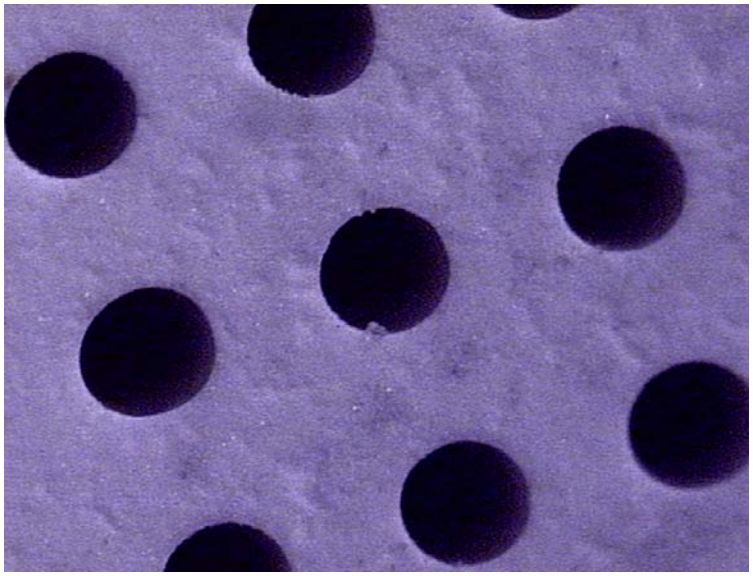

Fig. 6. Aluminum oxide microchannel plate with micro channel-holes (the final hole/channel

The mechanism of field dependent emission can be explained as follows. As a result of conventional secondary emission, the bombarding electrons tend to charge the surface of the dielectric (MgO) positively thus creating a high field across the film. Due to porosity most of the primary electrons can penetrate some distance into the volume of dielectric releasing secondary electrons. These secondary electrons in turn are accelerated towards the film and at sufficiently high field, electron avalanche will occur. In a MCP each channel acts as a continuous dynode that supports an avalanche multiplication of electrons when bias potential is applied across its length. A high secondary emission is achieved from insulators such as MgO because the wide band gap prevents internal secondary electrons from losing energy through collision with conduction electrons. This results in large escape depth and high secondary electron emission yield. Fig. 9 shows the escape depth of secondary electron emission for insulators of metallic oxides. It can be observed from the figure that MgO has highest escape depth which results in high secondary electron emission yield. Secondary electron emission yield is defined as the ratio of emitted secondary electrons to the input primary electrons.

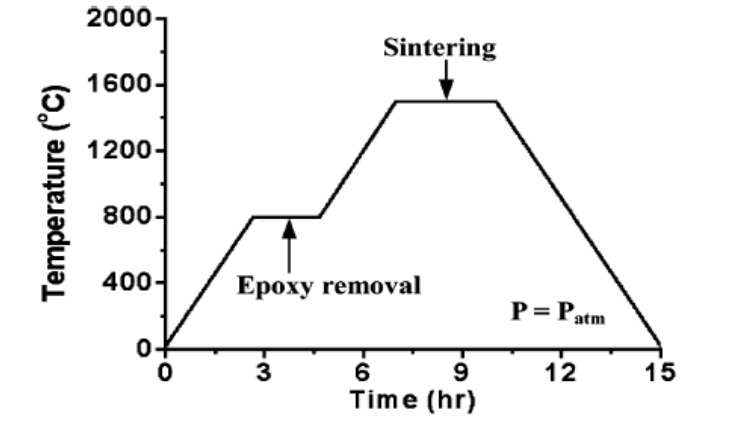

Fig. 7. Sintering cycle for alumina green body

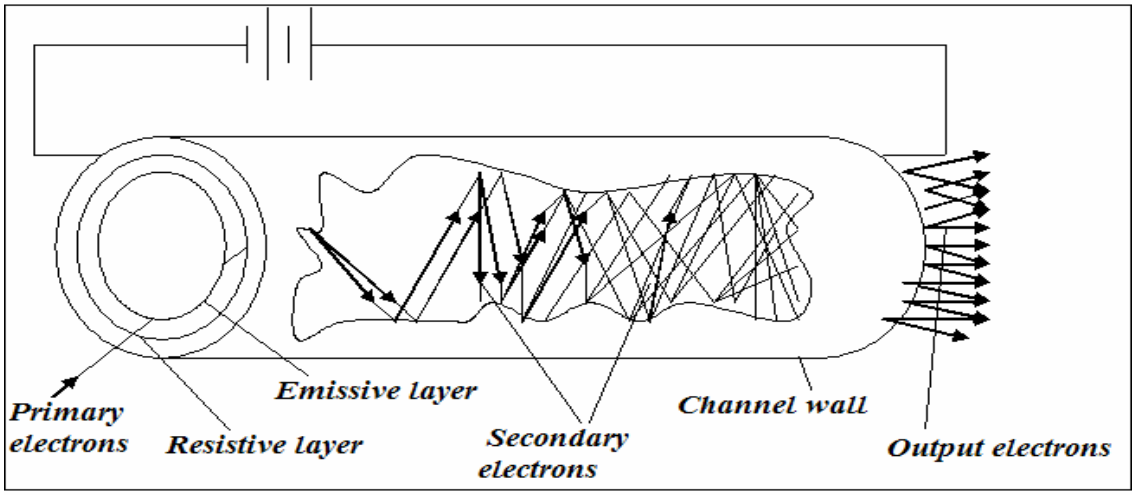

Fig. 8. Cross-sectional view of MCP channel

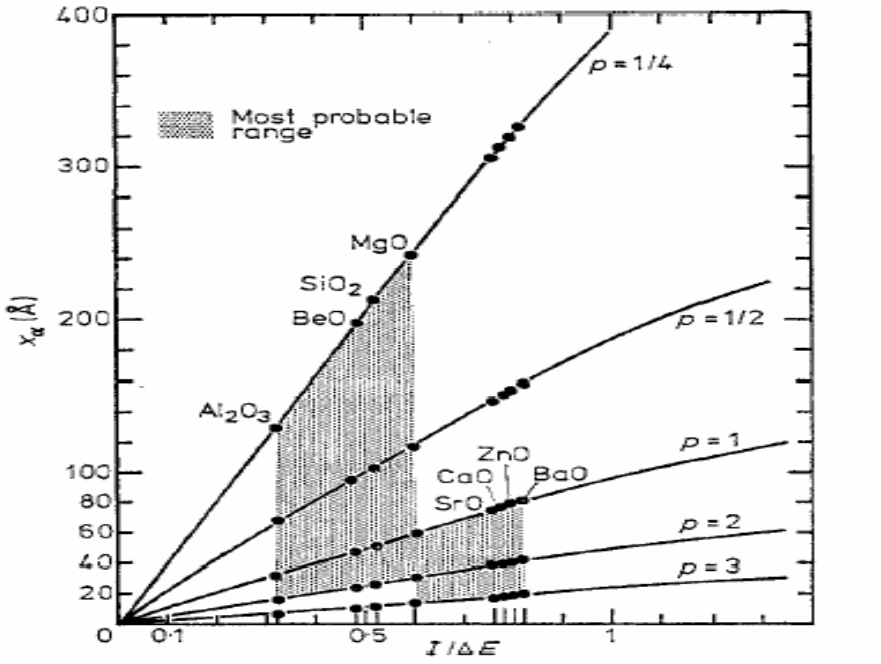

Fig. 9. Escape depth of secondary electron emission for insulators of metallic oxides with $x_\alpha = (393/p)(I/\Delta E)\ln(\Delta E/80\ I$. *(dotted lines show the range between maxima and minima of experimental results)* (x_α =escape depth) [18]

The secondary electron yield in MgO is influenced by the layer thickness, bias voltage, crystal quality and charging effect. The effect of crystal quality was explained by Cazaux et al, that the large decrease in secondary electron yield for polycrystalline insulators is caused by a reduced mean free path through scattering and trapping at defects [19]. *Space charge* can be

defined as “the electric charge carried by a cloud or stream of electrons or ions in vacuum of low gas pressure when the charge is sufficient to produce local changes in potential distribution”. Space charge limit is reached when the surface of MgO film reaches the same potential as the collector grid/anode. The charge built up can be dissipated by using short pulses. For insulators the pulse width is proportional to the charge deposited on the surface. Many researchers employ techniques such as pulse mode, [20, 21] preparation of cermet system [22] and application of thin layer [23] to overcome charging effect. For this project pulsed operation and control of MgO thickness will be used to overcome the charging effects.

3g. Field enhancement by space-controlled CNT using nanotemplate

To overcome the field screening effect and enhance the field concentration, we need to control the distance of carbon nanotubes. Therefore, to produce the most effective field emission cathodes, spacing controlled carbon nanotubes are needed. We have prepared AAO nano template through anodizing technique. Fig.10 shows the schematic of experimental setup of anodization and catalyst deposition along nano pore formed in nanotemplate.

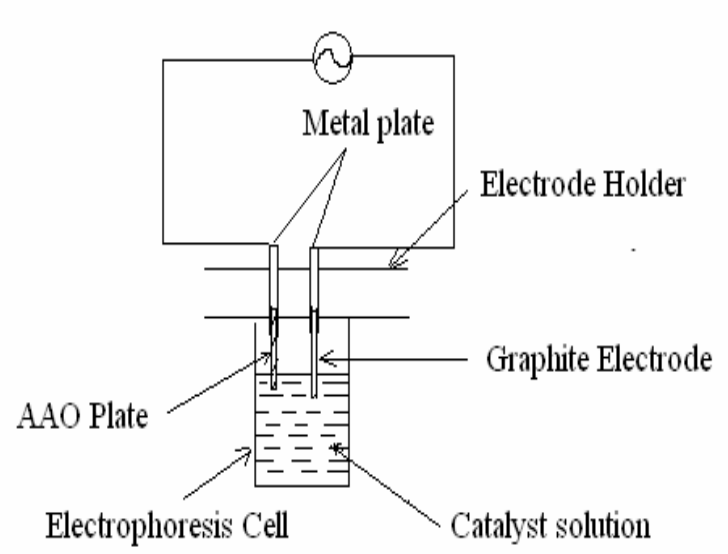

Fig. 10. Schematic of the deposition experimental set-up.

Catalyst solution consists of 60g ($CoSO_4 \cdot 7H_2O$), 10g of HBO_3 and 0.5g ascorbic acid in 250 ml of deionized water. AAO and graphite electrodes are immersed in the above solution. AC power supply is used for electrophoresis. Fig.11 shows the SEM image of AAO.

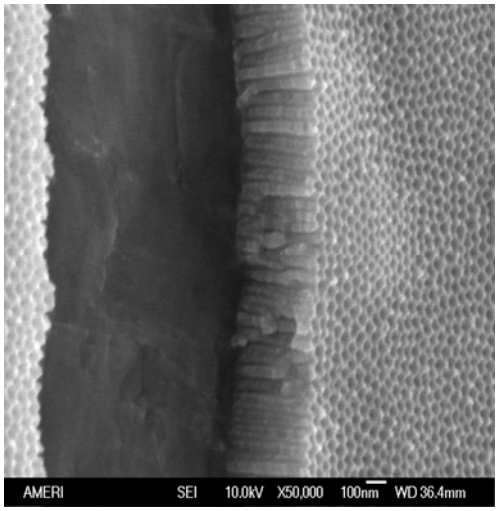

Fig. 11. SEM image of AAO (Diameter, length of the pores can be varied by varying AAO membrane thickness. This AAO nanotemplate will be used for growth of aligned CNT and micron size channel formation in Al_2O_3.

3h. Conclusions for Phase I nanotube cathode work

During the Phase I, achievements in nanotube cathode work include the following:

- Thin multi-wall nanotubes (MWNT's) were grown, which show
  - high emissivity;
  - low turn on voltage of 0.5 V/μm; and
  - good stability with an average emission current fluctuation of less than 2% at DC for over 2.5 hrs.
- A microchannel plate (MCP) was fabricated by drilling (mechanically) 50 μm diameter channels, which will be reduced to 10 μm after sintering (8% reduction) and deposition of Cu and MgO on the channel walls;
- A field emission measurement system for I-V characterization of carbon nanotubes, with DC and pulse power supplies, in a vacuum system capable of pressures below 10^{-7} Torr has been developed.
- Anodized aluminum oxide (AAO) nanotemplate synthesizing was achieved, and catalyst deposition in the AAO set-up has been developed.

3i. Review of goals for Phase I simulations of field emission cathode in RF gun

During Phase I, available steady-state and time-dependent computer codes were used to simulate the formation of a beam in a multi-cell rf gun, when a cathode having the capability of current density in the range beyond 1.0 kA/cm^2 is assumed to be installed in one face of the first half-cell of the gun. The rf geometry duplicated and then slightly modified that of the 6-MeV S-band rf gun which is available to Omega-P, that now employs a thermionic cathode. Results of the simulations are used to fashion the specifications for the cathode to be installed into the available rf gun. These specifications include current density, cathode geometry, and nearby cavity wall modifications so as to provide the lowest possible cathode current density variations, and low beam emittance, for a range of assumed emission phase windows.

3j. Results of simulation studies of field emission cathode in RF gun

Trajectory simulation studies for beam formation in the 2-1/2 cell rf gun were carried out, using both steady-state and time-dependent codes that have been used by Omega-P for several years in analysis of a wide variety of high-convergence electron gun and RF system designs. For the analysis here, it was assumed that the carbon nanotube field emission cold cathode with current multiplications channels could supply whatever current density was required, depending upon the voltage drop across the gap in the first half-cell cavity. Parameters of the cavities used for this analysis are shown in Table I. Electric fields in the first half-cell are shown in Fig. 12.

Table I. Parameters of the cavities of the RF gun.

	1st half-cell	full cells 2 and 3
quality factor Q	11,700	18,500
transit time factor T	0.94	0.77
shunt impedance R, MΩ	1.18	2.5
R/Q, Ohm	101	135
electric field enhancement ($\beta = 1$)	4	4.9

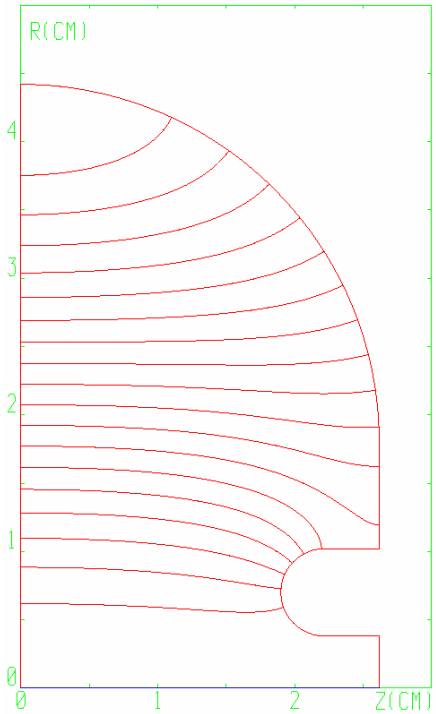

Fig. 12. RF electric field pattern in the first cell. Cathode surface location is at $z = 0$.

Steady-state beam trajectories in this cell are shown in Fig. 13, for an assumed cathode diameter of 1.0 mm. The calculated effective perveance K for this case was 0.025×10^{-6} A-V$^{-3/2}$, at a gap voltage of 180 kV. (K-values at other voltages will differ slightly, due to relativistic effects.)

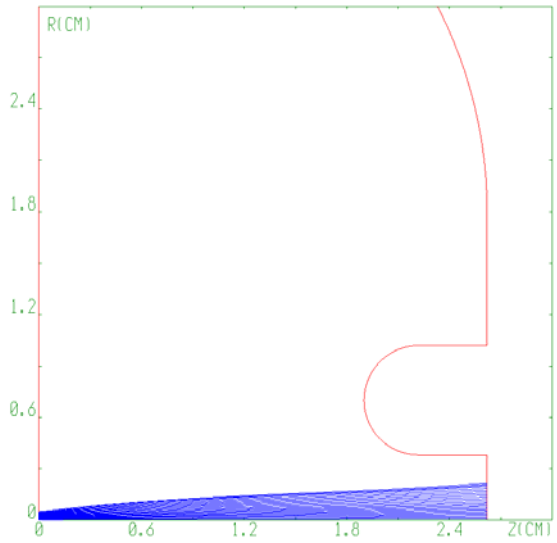

Fig. 13. Steady - state simulations of the beam dynamics in the first cell of the RF gun.

The required cathode current density for this beam is shown in Fig. 14. Clearly, the highly non-uniform distribution that was found is undesirable, as is the requirement for the cathode to supply a current density approaching 700 A/cm^2 at the cathode edge.

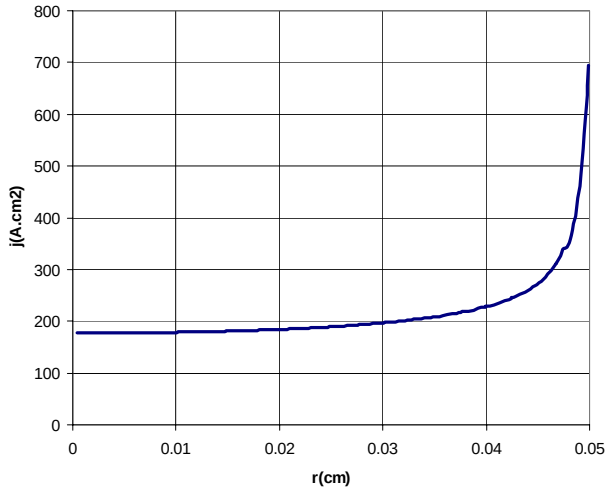

Fig. 14. Cathode loading for the case of unlimited emission and a flat back wall.

A remedy for the grossly non-uniform cathode current density is to introduce a "focus electrode," in the form of a slight 0.1 mm bulge or "funnel" in the wall contour, as shown in Fig. 15. Only the region near the cathode is shown in this figure, which has a different scale from that in Fig. 13. Beam trajectories are shown in Fig. 15; here the effective gun perveance is 0.017×10^{-6} A-V$^{-3/2}$, but the cathode current density as shown in Fig. 16 is now much more uniform, with a variation of about 30% with radius that is not atypical for conventional cathodes.

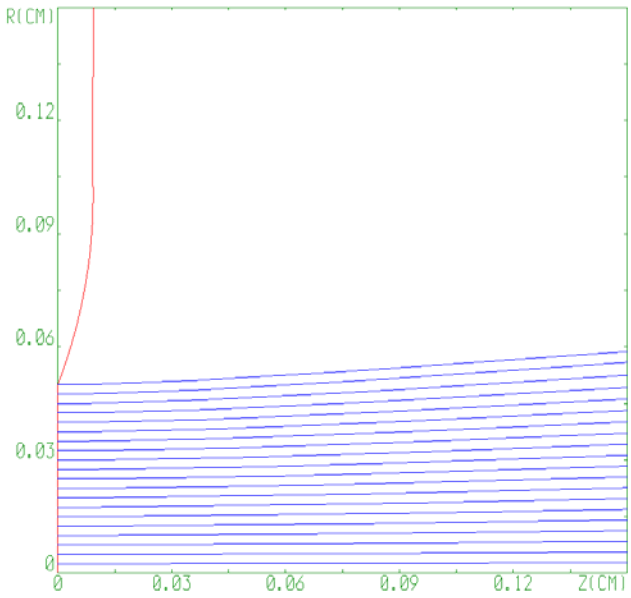

Fig. 15. Contour of a funnel near the cathode that improves the current density distribution.
In the case shown the funnel depth is 0.1 mm.
The surface electric field enhancement due to the funnel is only about 5%.

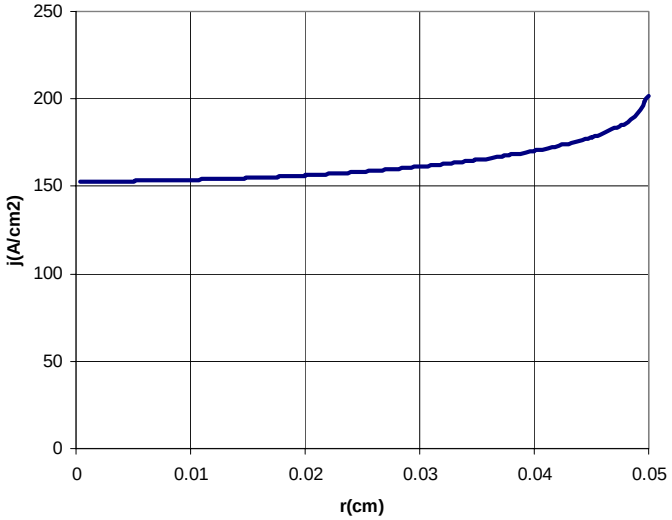

Fig. 16. Cathode loading in presence of the funnel shown in Fig. 15.

From this analysis, some orders-of-magnitude can be deduced, bearing in mind that more realistic results will be provided by time-dependent code analysis that will be discussed below. Gun parameters for a range of RF voltages V_1 on the first cell, and other quantities, can be found from the following simple relationships, where it is assumed that the fields in all three cavities are identical, that relative phases in all three cavities are optimal, that the first cell gap width d_1 is 2.6 cm, and that peak E-field enhancement k_1 is 4.0, that the cathode diameter is 1.0 mm, and other parameters are as in Table I.

energy gain in first (half-cell) cavity: T_1V_1 $= 0.94V_1$
energy gain in 2nd and 3rd cavities $2T_2V_1$ $= 1.54V_1$
energy gain in all three cavities $(T_1 + 4T_2)V_1$ $= V = 4.02V_1$
peak surface electric field E_{max} $T_1V_1k_1/d_1$ $= 1.446V_1$ (V/cm)
beam power $P_b = I_{av}V$ (approx.) $I_1V/2$ $= 2.0I_1V_1$ (W)
power dissipated in cavity P_{diss}
$= (V_1T_1)^2/2R_1 + 2(2V_2T_2)^2/2R_2 = (V_1T_1)^2/2R_1 + 4(V_1T_2)^2/R_2 = V^2/2R_{eff}$
effective shunt impedance $R_{eff} = (4.02)^2/[(T_1^2/R_1) + 8(T_2^2/R_2)]$ $= 6.11$ MΩ

Table II. Numerical values for gun and beam parameters.*

V_1 (kV)	I_1 (A)	$P = P_b + P_{diss}$ (MW)	V (MeV)	j (A/cm^2)	E_{max} (MV/m)
100	0.55	0.12	0.40	70	14.5
180	1.32	0.52	0.72	167	26.0
300	2.83	1.83	1.21	360	43.4
400	4.35	3.71	1.81	550	57.8
500	6.07	6.43	2.01	770	72.3
750	11.11	17.5	3.02	1410	108.5
1000	17.06	35.6	4.02	2170	144.6

*Neglecting the energy dependence of the transit time factors.

Clearly, if the cathode were not capable of an emission current density j as high as that shown in Table II, then this analysis would not apply. These estimates show the exceptional range of gun and beam parameters that would be possible if a current density in the kA/cm^2 range were available. Indeed, the realization of such a cathode is the main goal of this project.

Preliminary analysis of the RF gun with a 1.0-mm diameter high-current density cathode has been also carried out using a time-dependent code that includes space-charge fields. Figs. 17 and 18 show examples of the capability of this code. Fig. 17 shows the current at the cathode surface as as function of RF phase, for an RF gap voltage in the first half-cell cavity of 200 kV. For this case, the steady-state code predicted an average current of 1.54 A, a value within the range of the time-dependent solution. Reflected electrons are not taken into account in this portrayal.

This time-dependent analysis also allows "snapshots" to be obtained for space charge density in the RF gap at various times during the RF cycle. Fig. 18 is one such example. The arrows indicate the direction of space charge flow at the indicated times and locations. Snapshots are shown for different RF phases, where zero corresponds to the beginning of the accelerating phase. Electrons of previous bunches are not shown. The average pulse power of the accelerated beam after the 1st half-cell in this example is 120 kW, while the pulse power of the beam that reflects back to the cathode is 15 kW. In many RF guns, the reflected beam is caused to avoid returning to the cathode by imposition of a weak transverse dc magnetic field.

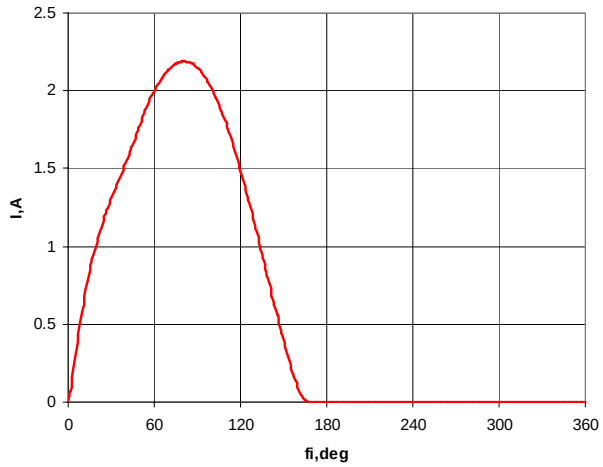

Fig. 17. Result of time-dependent simulations obtained using the code SMASON,* showing cathode current vs. rf phase for an RF gap voltage of 200 kV.
*A.V. Grudiev, D.G. Myakishev, V.P. Yakovlev, S. Luetgert, S. Krueger, "Numerical Simulation of a Gridded Inductive Output Amplifier", Proc. 1996 European Particle Accelerator Conference (EPAC'96), Barcelona, June 1996, pp. 1244-1246.

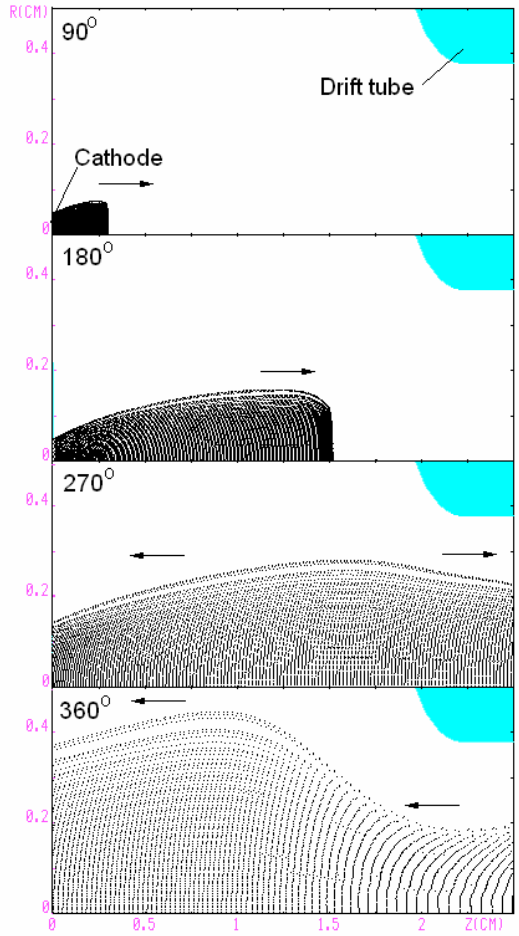

Fig. 18. Results of time-dependent simulations of space charge distributions in an RF gun.

While much analysis of space-charge flows and beam formation in multi-cell RF guns with high current-density cathodes remains to be done, the examples shown here demonstrate the capability of Omega-P to analyze such situations. As is seen from the 750 kV gap voltage case in Table II, it should be possible to produce a train of about 3000 ~11-A, 3-MeV, 100 ps bunches using about 17 MW of RF power; corresponding to 1.1 nC per bunch. Of course, focusing of these bunches (as at SSRL) using a combination of alpha-magnet and RF bunching can in principle produce few-ps >100 A bunches.

It was also planned to extend the steady-state analysis to cold-cathode guns for high-power RF amplifiers, such as klystrons and magnicons, that have accelerator applications, in anticipation that such cathodes could give improved beam quality and (eventually) increased reliability and cathode lifetime. This would have been especially significant for beams emitted from field emission cold CNT cathodes with current multiplication that also have gate electrodes at the base of the CNT's, and where ps-scale beam modulation or chopping becomes possible. That capability, once realized, would place the cathode in a class of its own, for use with a wide range of RF tubes, including high-power klystrons.

References

1. V.V. Zhirnov, C.L. Rinne, G. Wojak, J.J. Hren, "Analysis of high-current yield of diamond-based field emitters," Materials Research Society Symposium - Proceedings, 2000, v. 558, pp. 583-588.
2. W. Zhu, C. Bower, O. Zhou, G. Kochanski, S. Jin, "Large current density from carbon nanotube field emitters," *Appl. Phys. Lett.*, 1999, v. 75, pp. 873-875.
3. W. Yi, S. Yu, W. Lee, I. T. Han, T. Jeong, Y. Woo, J. Lee, S. Jin, W. Choi. "Secondary electron emission yields from MgO deposited on carbon nanotubes," *J. Appl. Phys.*, 2001, v. 89, pp. 4091-4095.
4. W. Yi, S. Jin, T. Jeong, J. Lee, S. Yu, Y. Choi, J. M. Kim, "Microchannel plate for high-efficiency field emission display," *Appl. Phys. Lett.*, 2000, v. 77, pp.1716-1718.
5. Robert J. Barker, Edl Schamiloglu (Editor), Robert Barker (Editor), "High-Power Microwave Sources and Technologies", IEEE, 2001, 528 p.
6. K.A. Dean and B.R. Chalamala, "Current saturation mechanisms in carbon nanotube field emitters," *Appl. Phys. Lett.*, 2000, v. 76, pp. 375-377.
7. W.B. Choi, D. S. Chung, J.H. Kang, H.Y. Kim, Y.W. Jin, I.T. Han, Y.H. Lee, J.E. Jung, N.S. Lee, G. S. Park, and J.M. Kim, "Fully sealed, high-brightness carbon nanotube field emission display", *Appl. Phys. Lett.* 75 3129 Nov. (1999).
8. W. Choi, B. Cheong, J. Kim, J. Ju, E. Bae, G. Chung, "Selective growth of carbon nanotube for nano-scale transistor," *Advanced Functional Materials*, 2003, v. 13, pp. 80-84.
9. C. Bower, W. Zhu, S. Jin, and O. Zhou, "Plasma-induced alignment of carbon nanotubes," *Appl. Phys. Lett.*, 2000, v. 77, pp. 830-832.
10. J.K. Ha, B.H. Chung, S.Y. Yan, J.O. Choi, "Drastic changes in the field emission characteristics of a Mo-tip field emitter array having PH3-doped a-Si:H as a resistive layer material throughout vacuum packaging processes in a field emission display," *J. Vac. Sci. Technol. B*, 2002, v. 20, pp. 2080-2084
11. J.K. Ha, B.H. Chung, S.Y. Han, J.O. Choi, H.G. Kim, "Novel resistive layer structure using via holes of an insulating interdielectric as a current path," *J. Vac. Sci. Technol. B*, 2001, v. 19, pp. 929-932.